

# Core Actuation Promotes Self-manipulability on a Direct-Drive Quadrupedal Robot

Jeffrey Duperret, Benjamin Kramer, and Daniel E. Koditschek

Department of Electrical and Systems Engineering, University of Pennsylvania, 200 South 33rd Street, Philadelphia, PA 19104

[jdup@seas.upenn.edu](mailto:jdup@seas.upenn.edu)

**Abstract.** For direct-drive legged robots operating in unstructured environments, workspace volume and force generation are competing, scarce resources. In this paper we demonstrate that introducing geared core actuation (i.e., proximal to rather than distal from the mass center) increases workspace volume and can provide a disproportionate amount of work-producing-force to the mass center without affecting leg linkage transparency. These effects are analytically quantifiable up to modest assumptions, and are demonstrated empirically on a spined quadruped performing a leap both on level ground and from an isolated foothold (an archetypal feature of unstructured terrain).

## 1 Introduction

The ability of legged robots to move through unstructured environments is critical to their practical utility in first-response and search-and-rescue operations. While recent work in the field has yielded a growing array of impressive legged platforms capable of steady-state dynamic behaviors over flat or modest terrain [1,2,3,4], there has been less focus on designing systems for locomotion in highly irregular environments. In particular, there has been relatively little experimental investigation into the locomotion prowess of non-conventional legged robot morphologies (departing from the traditional rigid-body-with-appendages framework) such as core actuation that are commonly seen in animals operating in unstructured terrain. Throughout this paper, the terms core and spine actuation should be taken to mean the introduction of actuated degrees of freedom proximal to rather than distal from the mass center.

Prior robotic literature on core actuation has largely focused on steady-state running gaits. Simulation studies of reduced-order models suggest that core actuation and compliance can provide increased speed, stability, and apex height while running [5,6,7]. Self-stabilizing gaits and decreased energetic cost of transport have been found with purely passive core compliance [8]. Experimental work involving core actuation has been more limited. The design of power-autonomous quadrupeds utilizing parallel stiffness is presented in [9] and [10]. Other experiments have suggested increased running speed [11] and gait transition stability [12]. Leaping from a crouched position with a parallel elastic-actuated spine was shown to increase leap energy in [13]. However, much more work is needed to provide designers with the quantifiable utility of core actuation or lack thereof, especially for the less-studied application of traversing irregular terrain.

This paper demonstrates two advantages of introducing core actuation to a direct-drive quadrupedal robot and experimentally quantifies the utility of this morphological design choice. Specifically, we demonstrate that—in inherently torque-limited, direct-drive machines [14,3] where workspace volume and force generation are competing, scarce resources for operation in unstructured environments—the addition of core actuation increases workspace volume without adversely affecting leg force generation. Additionally, using gearing in the spine allows an individual motor to provide the mass center a significantly higher amount of sustained, work-producing force than it can on a transmission-free leg, without affecting leg linkage transparency. We quantify both of these advantages and demonstrate them on a physical platform in a series of experiments involving leaping from level ground and an isolated foothold (an archetypal feature of unstructured terrain), a task requiring both large ground forces as well as a large workspace to facilitate balancing and self-manipulation [15].

## 2 Technical Approach: The Utility of Core Actuation

This section describes potential workspace volume and force production advantages of adding to a conventional sagittal-plane quadrupedal machine an actuated, revolute degree-of-freedom joint proximal to the mass center. Simplified models of quadrupedal platforms, such as the one depicted in Figure 1(a), often take the form of three-degree-of-freedom rigid bodies with common distances between the hips and mass center [16,17] and assume massless legs able to apply wrenches on the mass center when in contact with the ground subject to friction cone constraints. Following [6,7,8,9], we add core actuation to this model by introducing an actuated revolute joint to the body, depicted in Figure 1(b) (note that alternative formulations exist, such as [5]). Here we make the simplifying assumption that the parameters of each body segment are equal and that the mass center of each body segment is aligned with the leg hip, as is approximately true for the machine presented in Section 3. This model is used to analyze the experimental results given in Section 3.2.

We further limit our discussion to the class of direct-drive quadrupedal robots whose legs are actuated by DC electric motors (as exemplified by [3] whose drivetrain technology and principles of design are roughly adopted in the hips of our new, additionally spined robot to be introduced in the next section). These robots sacrifice potential motor output shaft torque for high actuator and leg linkage transparency, allowing motors to sense environmental forces and events like ground contact. Given such robots’ inherent torque limitations, it is desirable for the limb kinematics to produce high forces for given motor torques. Increasing force generation by decreasing lever arm length, however, trades away workspace size. Larger workspaces are highly beneficial in unstructured environments; they afford better access to intermittent footholds and improved body self-manipulation over a wider range of postures. A small workspace runs the risk of the robot becoming high-centered and losing balance on smaller footholds. In Appendix 1, we make explicit this trade-off confronting the designer when considering a simple scaling of a nominal leg linkage design.

Core actuation allows the body to move the leg hip with respect to the mass center, thereby augmenting the leg workspace volume. Consider the simplified case of an annulus leg workspace with inner radius  $r_1$  and outer radius  $r_2$ . The volume of the workspace is given by  $V = \pi(r_2^2 - r_1^2)$ . Assuming core bending can translate the center of this annulus a distance  $\bar{d}$  with respect to the mass center and that  $\bar{d} \geq r_1$ , the augmented workspace provided by core actuation is  $\bar{V} = \pi r_2^2 + 2r_2\bar{d}$ , a volume increase of  $2r_2\bar{d} + \pi r_1^2$ . This is depicted in teal in Figure 1. The utility of this added volume is empirically demonstrated on a spined robotic quadruped perching and leaping from an isolated foothold in Section 3.

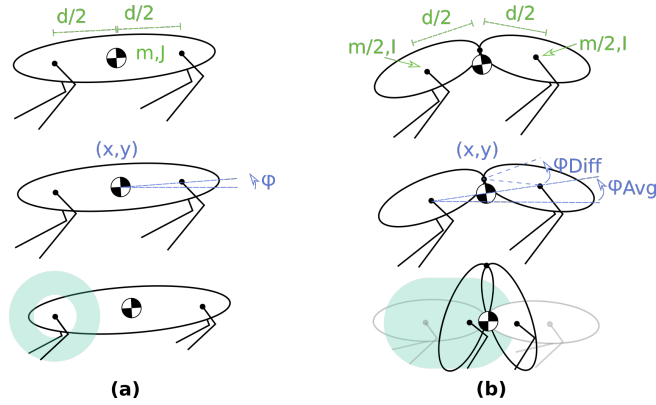


**Fig. 1.** (a) Simplified sagittal-plane three-degree-of-freedom model of a rigid body quadrupedal platform with massless legs. (b) Simplified sagittal-plane four-degree-of-freedom model of a spined quadrupedal platform possessing an actuated revolute joint proximal to the mass center. The models are parametrized by their mass, moment of inertia, and body segment length as shown in green. The state of the models is represented by the position and velocity of the mass center and the body segment pitch and angular velocity as shown in blue – for the spined model we choose to use the average body pitch and the difference between the pitch of the front and rear. Spine bending augments the nominal leg workspace (depicted in teal for a nominal annulus leg workspace) and provides an additional source of actuation to do useful work on the mass center. The core can be geared without affecting the direct-drive leg transparency.

Geared core actuation allows otherwise direct-drive machines to augment their inherently limited ability to exert large sustained forces on the environment. Since the gearing is proximal rather than distal to the mass center, it does not diminish the leg linkages transparency that allow sensing of environmental forces. For sufficiently high-powered operation, however, core actuation requires the legs to operate in a non-transparent region of their workspace as large forces generated on the ground by the core must be transmitted through the torque-limited legs to be usefully applied to the mass center. Explicitly, if  $F_{core}$  is the force generated by the core on a point contact with the ground through a static leg linkage, the leg motors must apply the torque  $Df^T(q)F_{core}$ , where  $Df(q)$  is the Jacobian of the leg's forward kinematic chain and  $q$  are the joint positions.

For sufficiently large force magnitudes this necessitates operating the legs near singularity, where a small singular value of  $Df(q)$  magnifies a component of the limited motor torque so the force generated at the core can transmit through the toe. This is a low-transparency regime of operation for the leg because external forces transferred to the motor are diminished along the direction corresponding to the small singular value of the linkage Jacobian. The robot, then, is able to operate in real-time in the continuum between two modes of operation: a low-force, high-transparency mode where the motors are capable of high-bandwidth environmental sensing, and a high-force, low-transparency mode where the geared core is able to perform significant work on the mass center.

We note that – although its quantification is outside the scope of the present work – the added revolute joint will increase platform mass and complexity on a physical machine. This added mass and complexity incurred should be weighed against the aforementioned advantages when considering a spined morphology.

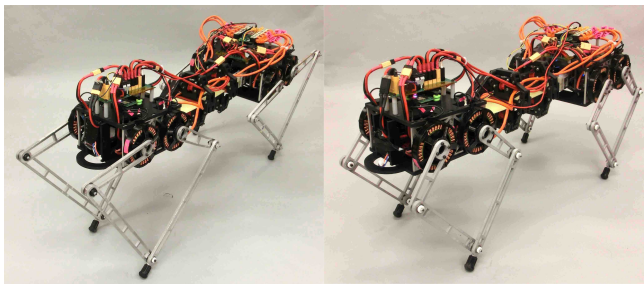


**Fig. 2.** The robot used in the experiments has a parallel elastic-actuated spine. A version of the robot with longer legs (left) is compared with a version with shorter legs (right) in leaping from an isolated foothold for the purpose of evaluating task sensitivity to workspace size. The ratio between the lengths of the distal and proximal link (shown in Figure 3) was chosen from numerical study to approximately maximize vertical leaping height over a range of scaling factors. The scaling factor of the distal and proximal links for the shorter legs was chosen near the smallest that allowed for balancing on the isolated foothold (specifically, to yield a minimal but non-empty intersection of the front and rear leg workspaces without core bending, allowing both legs to “grasp” the same point), and for the longer legs was chosen to be 1.5 times the shorter legs—a large enough increase to reasonably expect a significant performance difference compared to the shorter legs while keeping the extended leg length less than the hip-to-hip length as we were wary of avoiding excessive pitching when accelerating from rest caused by long legs [18].

### 3 Experiments and Results

This section introduces a robotic quadrupedal platform utilizing core actuation and quantifies advantages provided by the core in leaping experiments.

#### 3.1 Experimental Setup

The robot used to perform the experiments is shown in Figure 2. It consists of a front and rear body segment connected by a parallel elastic-actuated spine. The

legs are 2-degree-of-freedom 5-bar linkages driven by 2 direct-drive TMotor U8-16<sup>1</sup> brushless DC motors as shown in Figure 3 and using drive electronics derived largely from those detailed in [19]. The spine is a minor variation on the design documented in [10], differing from its predecessor by using a belt drive instead of cable drive and by using different motors. The spine’s belt drive, running across the length of the spine, is actuated by a pair of coaxially-mounted U8-16 motors in parallel configuration housed in the rear body segment. A sprocket in the rear body segment connects these motors to the belt and accounts for the spine gearing. A fiberglass plate provides parallel compliance and constrains the bending motion. As this work does not focus on the energetic contribution of this parallel compliance, a thin fiberglass plate storing minimal elastic energy was used. The spine motors pull on the belt against a fixed sprocket on the front of the robot, causing upward or downward spine bending. Vertebrae affixed around the fiberglass plate act as guides for the belt (as introduced in [10]), and spring-loaded tensioners compensate for loss of tension during bending. Control is performed on-board the robot, using an STM32F3<sup>2</sup> microcontroller to command the 10 motors through custom motor controllers capable of providing up to 43A of current per motor. Power is provided by an on-board 3S lithium polymer battery. The only sensors aside from magnetic encoders on the motor shafts are 2 InvenSense MPU6000<sup>3</sup> IMUs that are used to estimate the orientation of the front and rear body segments. The position and orientation of the front and rear body segments were tracked during the experiments using a 22-camera Qualisys<sup>4</sup> motion capture system. This data was fit to the reduced-order, sagittal plane model depicted in Figure 1 to ascertain the mass center trajectory and body energy.

To physically demonstrate the advantages of the spine, two leaping experiments were performed. In the first, the robot executed leaps off of a 20 cm-tall, 9 cm-wide perch as depicted in Figure 4 to illustrate the sensitivity to workspace size when operating on isolated footholds. These leaps were performed with the longer legs shown in Figure 3 without spine bending to illustrate task performance without workspace constraints, and with shorter legs to introduce workspace constraints. The minimum and maximum longer leg lengths are 0.141m and 0.447m, respectively, while the minimum and maximum shorter leg lengths are 0.087m and 0.296m, respectively. However, due to the complicated geometry of the workspace volume these lengths are obtainable only when the toe is vertically aligned with the hip. Spine bending was then used with the shorter legs to evaluate if the workspace benefit provided by the spine yielded a significant performance advantage. Each leaping configuration (long legs without spine bending, short legs without spine bending, and short legs with spine bending) was run 6 times using the feed-forward control strategy detailed below. In the second experiment, the robot leapt forwards from level ground using the

<sup>1</sup> <http://www.rctigermotor.com/>

<sup>2</sup> [http://www.st.com/content/st\\_com/en/products/microcontrollers.html](http://www.st.com/content/st_com/en/products/microcontrollers.html)

<sup>3</sup> <https://store.invensense.com/>

<sup>4</sup> <http://www.qualisys.com/>

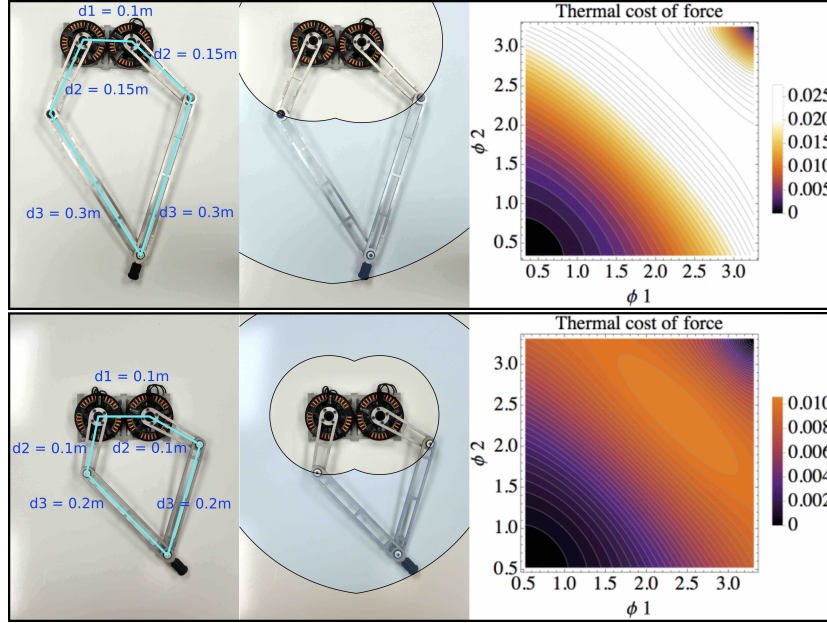


**Fig. 3.** The leg kinematics (left) are shown for 2 different sets of linkage lengths used in the experiments. The longer legs have a larger workspace (middle) while the shorter legs are able to generate higher forces for a fixed motor torque (right), as indicated by the smaller average of the squared singular values of the forward kinematic Jacobian for given motor shaft angles  $\phi_1, \phi_2$ , or equivalently, thermal cost of force [14, page 48] for a normalized motor constant. The depicted workspace and singular value results assume an end effector located where the links  $d_3$  are connected.

shorter leg configuration with and without spine bending to quantify the sustained forces generated by the spine. Each experiment was conducted 6 times.

In each trial, the feed-forward leaping strategy consisted of forcefully extending the front and rear legs. The magnitude of the vector of motor torques generated by each leg module was maximized with respect to the sup-norm torque-limit constraint imposed by the power electronics. The direction of this vector was chosen so that the ground reaction force vector created at the toe was approximately 45 degrees from vertical. A modification to this strategy granting better performance was used on level ground, where the rear legs pushed directly backwards at 0 degrees with respect to horizontal while the front extended, then switched to the nominal 45 degree ground reaction force vector, and then to a nearly vertical force vector as they neared the end of their extension<sup>5</sup>. When spine bending was used, the spine motors applied their maximum torque to extend the spine after a short time delay to allow the rear legs to acquire good traction and for the front to extend. If spine bending was not used, the spine motors worked to keep the spine in a straight configuration during the duration of the leap.

<sup>5</sup> This imparted a pitching moment on the body that improved the landing.

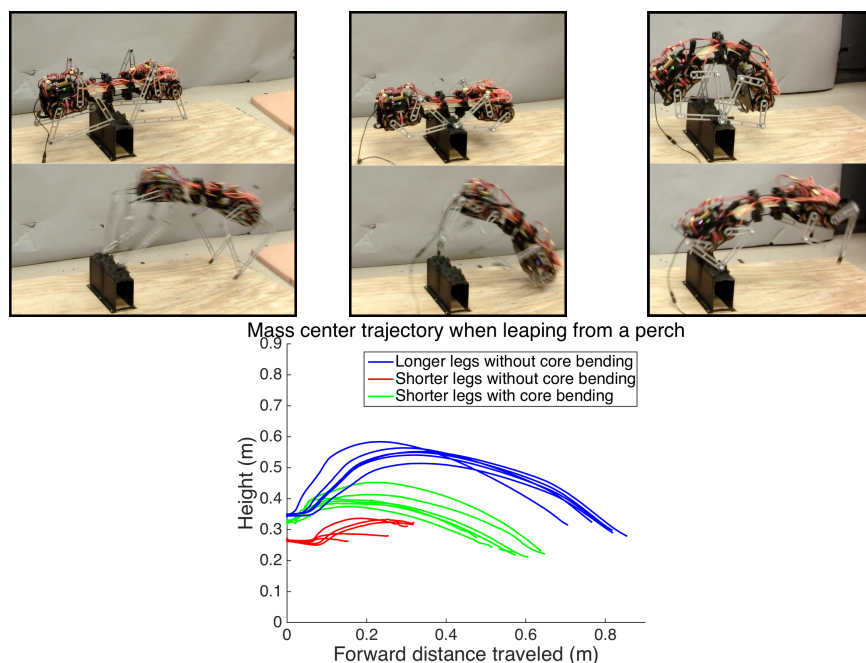


**Fig. 4.** Leaping off a 9 cm-wide isolated foothold succeeded without core bending using longer legs (top-left, bottom blue), failed without core bending using shorter legs (top-center, bottom red), and succeeded with core bending using shorter legs (top-right, bottom green). These qualitative results—further described in Section 3.2—suggest that core bending provides a benefit to the robot’s kinematic workspace, allowing a successful leap using shorter legs than would be possible without core bending.

### 3.2 Experimental Results

**Perch Leaping Results** Balancing on and leaping from a 20 cm-tall, 9 cm-wide foothold was successful using the longer legs of Figure 3 without core bending. With shorter legs and without core bending, the robot balanced on the foothold despite all four legs being near the edge of their workspace, but attempts at leaping failed. Specifically, the front legs were unable to push backwards during the leap, and any forward motion of the body moved the foothold out of the front legs’ workspace. The result was that the robot cantilevered on the back legs and pitched downwards, causing the front body segment to impact the ground. On the other hand, with shorter legs and with core bending the robot successfully leaped, aided by the increased workspace volume provided by the spine bending. The mass center trajectories during the leaps are plotted in Figure 4. The robot achieved an average horizontal leap distance of 0.80 m using the long legs without the spine and 0.59 m using the short legs with the spine. We attribute this difference to several contributing factors. First, the longer legs provide a larger kinematic extension than the shorter legs, which directly increases the distance they push the mass center. Second, the analysis in Section 3.3 indicates that the spine successfully augments the workspace but the longer legs still provide a

greater contribution to accomplish the workspace-sensitive task. Finally, we still do not fully understand how to apply the entire energetic contribution of the spine to the mass center using hand-tuned leaps from level ground as discussed in Section 3.3—a difficulty that is only compounded when leaping from the perch.

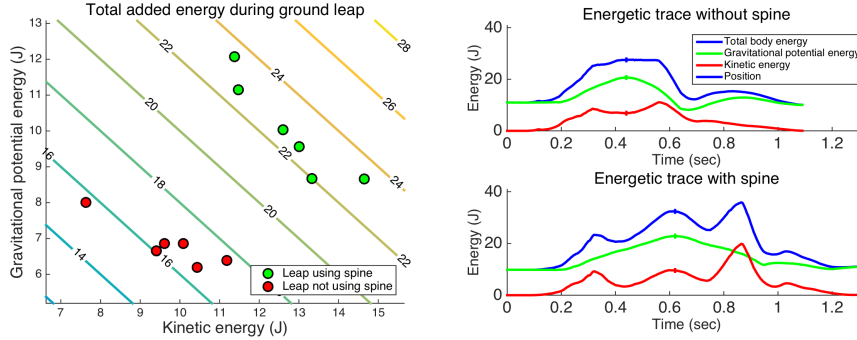


**Fig. 5.** Leaping from the ground with and without spine bending using an otherwise identical feed-forward control scheme shows that the spine motors add on average 5.7 J to the body energy [13] (discounting the 0.5 J stored in initial spine elastic potential energy). The body energy added is calculated by subtracting the energy at the leap height apex—indicated by a vertical tick in the sample energetic traces shown in the right figure—from the starting energy. These results show the spine motors add a disproportionate amount of work (36% more) during the leap on a per-motor basis as compared with the leg motors due to their gearing.

**Ground Leaping Results** Leaping was successful on flat ground using the shorter leg configuration both with and without spine bending as shown by the energetic results in Figure 5. These energetic results were calculated from the *extrinsic body energy* of the robot, the sum of the mass center’s kinetic and gravitational potential energy relative to a simplified Lagrangian model, as documented in [13]. Leaping aided by spine bending added an average of  $22.8 \pm 0.5$  J to the body (an average of 22.3 J when discounting the elastic potential energy separately measured to be stored in the spine’s fiberglass plate bending) and leaping with an identical strategy but without bending the spine added an average of  $16.6 \pm 0.7$  J to the body, 6.2 J less than with spine bending. After discounting the elastic potential energy stored in the spine, we attribute the 34% increase in energy when using the spine to the spine motors, since they are the only other source of work available.

### 3.3 Experimental Insights Into Core Actuation Utility

**Core Workspace Benefit** The results of the experiments in leaping from a small isolated foothold in Section 3.2 qualitatively indicate that the core is able to increase the legs’ workspace with respect to the mass center to accomplish a



useful task. This benefit allows for the leap to be completed using shorter legs capable of generating higher forces—as indicated by the singular values of Figure 3—than if no spine was used. Analytically quantifying the increased workspace conferred by the spine is confounded by the complex workspace geometry of the legs and their lack of rotational symmetry. We can estimate this increase, however, by making the approximation  $d_1 = 0$  for the leg kinematics shown in Figure 3 such that the linkage becomes the annulus analyzed in Section 2 with an inner radius  $r_1 = d_3 - d_2$  and outer radius  $r_2 = d_3 + d_2$ . Under this approximation, the longer leg linkage represents a scaling of the shorter leg linkage by a scaling factor of 1.5. The spine can move one hip a distance  $\bar{d} = 10\text{cm}$  with respect to the center of mass, satisfying  $\bar{d} \geq r_1$  for the shorter legs. Thus, using the results of Section 2, the volume for the shorter-legs-without-spine configuration is  $0.25\text{m}^2$ , for the shorter-legs-plus-spine configuration is  $0.34\text{m}^2$ , and for the longer legs is  $0.57\text{m}^2$ . The perching experiments show that—while the volumetric benefit provided by the spine is not greater than that provided by the longer legs—this approximately 36% increase in workspace volume provided by the core allows successful self-manipulation on the perch.

**Geared Core Work Production** The 34% increase in body energy provided by the spine motors during the ground leaping experiments show that the spine motors add a disproportionate amount of work during the leap on a per-motor basis as compared with the leg motors. By commanding the spine motors to do useful work during the leap, the number of work-producing motors increased by 25% from 8 to 10. If the spine motors had the same energetic effect as an average leg motor, then one could reasonably assume a 25% increase in leaping body energy by using the spine.<sup>6</sup> Instead, by increasing the body energy by 34%, each spine motor did 36% more work on the mass center than the average leg motor did. This is made possible by the spine gearing which allows the spine motors to rotate through a much greater angular displacement than the leg motors ( $2.6\pi$  radians in the spine versus an average less than  $\pi$  radians in the legs) while maintaining a similar torque.<sup>7</sup>

Under ideal conditions, the spine could likely perform much better. Theoretically, if the leg motors were used to their full potential at their low-speed

<sup>6</sup> This assumes that all the leg motors operate at near constant torque, which is often a reasonable assumption for direct-drive legged-robot motors given their typical low-speed, torque-limited regime of operation. In these experiments, the motor torque is limited by the power electronics’s 43A maximum current output, so a U8-16 motor being driven at 12V hits the speed-torque curve and becomes power-limited when rotating faster than 42 rad/sec. The maximum angular velocity observed on the leg motors was less than 30 rad/sec, so the leg motors never leave their low-speed torque-limited regime of operation.

<sup>7</sup> Unlike the legs, the spine motors see speeds as high as 62 rad/sec and thus transition from being torque-limited by the power electronics to being limited by the speed-torque curve. At such high speeds, the maximum torque output is 76% of the maximum leg torque output. Increasing the voltage driving the motors would diminish this torque loss.

torque-limited regime of operation they would each do  $\pi\tau$  Joules of work in a leap or stride, assuming operation at a torque limit of  $\tau$  over an angular displacement of  $\pi$  radians. With 8 leg motors used on a quadrupedal machine this gives  $8\pi\tau$  Joules of available work. Adding 2 spine motors capable of a conservative angular displacement of  $2.5\pi$  radians in the same low-speed torque-limited regime of operation would then increase the total maximum available work in a leap<sup>8</sup> to  $13\pi\tau$ , a 62.5% increase in body energy in which each spine motor does 2.5 times more work on the mass center than a leg motor. Our spine experiments saw only slightly more than half of this theoretical increase in body energy, indicating that further efforts toward improving the leaping controllers will be required in order to fully exploit the potential energetic benefits of core actuation.

## 4 Conclusions and Future Work

In direct drive machines, the addition of core actuation increases workspace volume and—with gearing—can allow the spine motors to do a disproportionately large amount of work on the mass center as compared with leg motors without negatively affecting the leg linkage transparency. These effects are analytically quantifiable up to modest assumptions and approximations, and were demonstrated empirically on a spined quadruped performing a leap both on level ground and from an isolated foothold. These results indicate that core actuation can provide designers with specific advantages (if worth the increased mass and complexity) for inherently torque-limited, direct-drive machines where workspace volume and force generation are competing scarce resources for operation in unstructured environments.

Improved balance and leap performance on isolated footholds is just one example of many possible uses of core actuation in unstructured terrain. Future work now in progress seeks an experimentally-validated, reduced-order model of quadrupedal core actuation applicable to both steady-state and transitional tasks that we hope will be a first step towards quantifying and promoting new sharper hypotheses concerning the potential utility of core actuation in robotic legged locomotion.

**Acknowledgments.** This work is supported by the National Science Foundation under both the Graduate Research Fellowship Grant No. DGE-0822 and CDI-II CABiR (CDI 1028237), as well as by the Army Research Laboratory under Cooperative Agreement Number W911NF-10-2-0016.

## References

1. S. Seok, A. Wang, M. Y. Chuah, D. J. Hyun, J. Lee, D. M. Otten, J. H. Lang, and S. Kim, “Design principles for energy-efficient legged locomotion and imple-

<sup>8</sup> This benefit is doubled when accounting for the fact that the spine can both extend on liftoff and retract on landing to perform useful work over the course of a leap or stride, unlike a leg motor.

- mentation on the mit cheetah robot,” *IEEE/ASME Transactions on Mechatronics*, vol. 20, no. 3, pp. 1117–1129, 2015.
2. A. Hereid, J. Van Why, S. Kolathaya, J. W. Hurst, M. S. Jones, and A. D. Ames, “Dynamic multi-domain bipedal walking with a trias through slip based human-inspired control,” in *HSCC 2014 - Proceedings of the 17th International Conference on Hybrid Systems: Computation and Control (Part of CPS Week)*, 2014, pp. 263–272.
  3. G. Kenneally, A. De, and D. E. Koditschek, “Design principles for a family of direct-drive legged robots,” *IEEE Robotics and Automation Letters*, vol. 1, no. 2, p. 900907, Jul 2016. [Online]. Available: <http://ieeexplore.ieee.org/stamp/stamp.jsp?arnumber=7403902>
  4. “Boston dynamics,” <http://www.bostondynamics.com>.
  5. Q. Zhao, H. Sumioka, K. Nakajima, X. Yu, and R. Pfeifer, “Spine as an engine: Effect of spine morphology on spine-driven quadruped locomotion,” *Advanced Robotics*, vol. 28, no. 6, pp. 367–378, 2014.
  6. S. Pouya, M. Khodabakhsh, A. Sprwitz, and A. Ijspeert, “Spinal joint compliance and actuation in a simulated bounding quadruped robot,” *Autonomous Robots*, pp. 1–16, 2016, article in press.
  7. U. Culha and U. Saranlı, “Quadrupedal bounding with an actuated spinal joint,” in *Proceedings - IEEE International Conference on Robotics and Automation*, 2011, pp. 1392–1397.
  8. Q. Cao and I. Poulakakis, “Quadrupedal bounding with a segmented flexible torso: Passive stability and feedback control,” *Bioinspiration and Biomimetics*, vol. 8, no. 4, 2013.
  9. G. A. Folkertsma, S. Kim, and S. Stramigioli, “Parallel stiffness in a bounding quadruped with flexible spine,” in *IEEE International Conference on Intelligent Robots and Systems*, 2012, pp. 2210–2215.
  10. J. L. Pusey, J. M. Duperret, G. C. Haynes, R. Knopf, and D. E. Koditschek, “Free-standing leaping experiments with a power-autonomous elastic-spined quadruped,” in *SPIE Defense, Security, and Sensing*, vol. 8741. International Society for Optics and Photonics, 2013, pp. 87 410W–87 410W.
  11. M. Khoramshahi, A. Sprowitz, A. Tuleu, M. N. Ahmadabadi, and A. J. Ijspeert, “Benefits of an active spine supported bounding locomotion with a small compliant quadruped robot,” in *Proceedings - IEEE International Conference on Robotics and Automation*, 2013, pp. 3329–3334.
  12. K. Tsujita, T. Kobayashi, T. Inoura, and T. Masuda, “Gait transition by tuning muscle tones using pneumatic actuators in quadruped locomotion,” in *2008 IEEE/RSJ International Conference on Intelligent Robots and Systems, IROS*, 2008, pp. 2453–2458.
  13. J. M. Duperret, G. D. Kenneally, J. L. Pusey, and D. E. Koditschek, “Towards a comparative measure of legged agility,” in *International Symposium on Experimental Robotics*, Marrakech/Essaouira, Morocco, June 2016.
  14. H. Asada and K. Youcef-Toumi, *Direct-drive robots: theory and practice*. MIT press, 1987.
  15. A. M. Johnson and D. E. Koditschek, “Legged self-manipulation,” *IEEE Access*, vol. 1, pp. 310–334, May 2013.
  16. H.-W. Park, P. M. Wensing, S. Kim *et al.*, “Online planning for autonomous running jumps over obstacles in high-speed quadrupeds,” in *Proceedings of the Robotics: Science and System (RSS)*, June 20–22 2015, p. (to appear).

17. I. Poulakakis, J. A. Smith, and M. Buehler, “Experimentally validated bounding models for the scout ii quadrupedal robot,” in *Proceedings - IEEE International Conference on Robotics and Automation*, vol. 2004, 2004, pp. 2595–2600.
18. S. B. Williams, H. Tan, J. R. Usherwood, and A. M. Wilson, “Pitch then power: Limitations to acceleration in quadrupeds,” *Biology Letters*, vol. 5, no. 5, pp. 610–613, 2009.
19. A. De and D. E. Koditschek, “The Penn Jerboa: A platform for exploring parallel composition of templates,” Online: <http://arxiv.org/abs/1502.05347>, [http://repository.upenn.edu/ese\\_reports/16](http://repository.upenn.edu/ese_reports/16), Tech. Rep., Feb 2015, arXiv:1502.05347.
20. R. M. Murray, Z. Li, S. S. Sastry, and S. S. Sastry, *A mathematical introduction to robotic manipulation*. CRC press, 1994.

## Appendix 1: Analytic Leg Force Generation Versus Workspace Volume Trade-off via Linkage Scaling

We explicitly show the trade-off between leg force generation and workspace volume confronting the designer by considering a simple scaling of a nominal leg linkage design by a scaling factor  $\lambda$ , assuming a fully actuated leg interacting with the ground through a point contact. Let the forward kinematic map of the nominal leg linkage with a point toe and origin at the hip be given by  $f : Q \rightarrow \mathbb{R}^n$ , where  $q \in Q$  denotes the actuated joint positions. Consider a uniform scaling transformation applied to this linkage, scaling the length of all vectors by a factor of  $\lambda \in \mathbb{R}^+$ , and let  $f_\lambda(q) := \lambda f(q)$  denote the forward kinematic map of the scaled linkage. The nominal leg linkage has a workspace volume given by  $V := \int_{f(Q)} \Omega$ , where  $\Omega$  indicates the standard volume form on  $\mathbb{R}^n$  [20]. The forces  $F$  generated at the toe from motor torques  $\tau$  is then given by  $F(q) := Df^{-T}(q)\tau$  assuming the leg linkage is not at singularity, where  $Df := \frac{\partial f}{\partial q}$ . Denoting the workspace volume of the scaled linkage by  $V_\lambda := \int_{f_\lambda(Q)} \Omega$  and the forces generated at the toe by  $F_\lambda(q) := Df_\lambda^{-T}(q)\tau$ , we have that

$$\begin{aligned} V_\lambda &= \int_{\lambda f(Q)} \Omega = \int \dots \int_{\lambda f(Q)} dx_1 \dots dx_n = \int \dots \int_{f(Q)} \lambda dy_1 \dots \lambda dy_n \\ &= \lambda^n \int \dots \int_{f(Q)} dy_1 \dots dy_n = \lambda^n V \end{aligned}$$

and

$$F_\lambda(q) = (\lambda Df(q))^{-T} \tau = \frac{1}{\lambda} Df^{-T}(q) \tau = \frac{1}{\lambda} F(q),$$

so that increasing scale has the dual effect of decreasing end effector force magnitude for a given motor torque vector while increasing workspace volume.<sup>9</sup>

<sup>9</sup> An established metric for evaluating the ability of a direct-drive limb to generate forces is thermal cost of force (for a normalized motor constant) given by the mean of the squared singular values of the forward kinematic Jacobian [14, page 48], [3]. As shown in the analysis above, in general smaller singular values are achievable by decreasing the length of lever arms in the (possibly parallel) kinematic chain to gain a greater mechanical advantage.